Protein Science (1993), *2*, 448-458. Cambridge University Press. Printed in the USA.

Crystal structure of human annexin I at 2.5 Å resolution

XIANGWEI WENG,[1,3] HARTMUT LUECKE,[4] IN SUNG SONG,[5] DOE SUN KANG,[5] SUNG-HOU KIM,[2,3] AND ROBERT HUBER[4]

[1] Department of Molecular and Cell Biology, [2] Department of Chemistry, and
[3] Lawrence Berkeley Laboratory, University of California, Berkeley, California 94720
[4] Max-Planck-Institut für Biochemie, D-8033 Martinsried, Germany
[5] Asan Institute for Life Sciences, College of Medicine, University of Ulsan, Seoul 134-600, Korea

(RECEIVED October 30, 1992; REVISED MANUSCRIPT RECEIVED January 6, 1993)

Abstract

cDNA coding for N-terminally truncated human annexin I, a member of the family of Ca^{2+}-dependent phospholipid binding proteins, has been cloned and expressed in *Escherichia coli*. The expressed protein is biologically active, and has been purified and crystallized in space group $P2_12_12_1$ with cell dimensions $a = 139.36$ Å, $b = 67.50$ Å, and $c = 42.11$ Å. The crystal structure has been determined by molecular replacement at 3.0 Å resolution using the annexin V core structure as the search model. The average backbone deviation between these two structures is 2.34 Å. The structure has been refined to an *R*-factor of 17.7% at 2.5 Å resolution. Six calcium sites have been identified in the annexin I structure. Each is located in the loop region of the helix-loop-helix motif. Two of the six calcium sites in annexin I are not occupied in the annexin V structure. The superpositions of the corresponding loop regions in the four domains show that the calcium binding loops in annexin I can be divided into two classes: type II and type III. Both classes are different from the well-known EF-hand motif (type I).

Keywords: annexin; calcium binding protein; crystal structure; lipocortin; phospholipase inhibitor

Annexins are a widely distributed family of homologous amphipathic cytosolic proteins that bind to phospholipids and membranes in a Ca^{2+}-dependent manner. Some members function as inhibitors of inflammation and coagulation. They interact with cytoskeletal proteins and participate in membrane fusion and exocytosis. Some members also have voltage-dependent calcium channel activity (Crompton et al., 1988; Flower, 1988; Klee, 1988; Karshikov et al., 1992).

Corticosteroid hormones (glucocorticoids) such as cortisone are thought to act as antiinflammatory drugs by inducing white blood cells to synthesize and/or secrete annexin I as a local chemical mediator. Annexin I inhibits the activity of phospholipase A_2 in the first step of the eicosanoid synthesis pathway, in which membrane lipids are degraded through arachidonic acid into inflammation mediating eicosanoids (Flower, 1988; Peers & Flower, 1990).

Reprint requests to: Sung-Hou Kim, Melvin Calvin Lab, University of California, Berkeley, California 94720.

All annexins contain either four or eight copies of a homologous 70-amino acid repeat. The amino termini of the annexins are quite diverse, and among them, annexin I has the longest with 42 residues. Experiments have shown that the amino-terminal domain of annexin I is the site of tyrosine phosphorylation by the epidermal growth factor receptor kinase (Glenney & Tack, 1985; Haigler et al., 1987) and that it has the ability to modulate the protein's affinity for Ca^{2+} (Glenney & Zokas, 1988; Ando et al., 1989). Annexin II also has a long (33 residues) amino terminus. It has been found that both annexin I and II promote aggregation of phosphatidylserine vesicles at low micromolar Ca^{2+} concentrations, whereas other annexins do not (Ernst et al., 1991).

We describe here the crystal structure of the calcium-bound form of human annexin I lacking the N-terminal 32 residues, and compare it with the annexin V structure (Huber et al., 1990a,b, 1992). Similarities and differences between the two proteins and new features are described. In order to facilitate structural comparisons, the annexin I sequence was aligned with annexin V. In accordance

with the annexin V sequence numbering, the original annexin I sequence 33–346 has been renumbered as 6–319 here.

Results

Structure determination by molecular replacement

The diffraction data were collected with 1.00-Å synchrotron radiation at the Photon Factory in Tsukuba, Japan, on a macromolecular Weissenberg camera (Sakabe, 1983) using Fuji Type II phosphor imaging plates. The plates were read on a Fuji BA100 scanner with a nominal pixel size of 100 μm. The digitized images were reduced to structure factors, merged, and scaled into a unique data set with the program WEIS (Higashi, 1989). Relevant statistics are shown in Table 1.

The crystal structure of annexin I was solved by the molecular replacement method using the program XPLOR (Brünger, 1990b). The search model was based on the crystal structure of annexin V (Huber et al., 1990a,b). Sequence alignment of these two proteins shows that, excluding the N-terminal extra 27 residues in annexin I, they have 43% sequence identity (Huber et al., 1992). The search model was built by removing the amino-terminal segment of annexin V and changing the nonhomologous residues to alanines.

Rotation searches were performed using a real-space Patterson search method (Rossmann, 1972; Huber, 1985). The model Patterson map was calculated by placing the molecule into an orthogonal box with 150-Å cell edges, and calculating the Patterson coefficients. The grid spacing used for both rotated and stationary Patterson maps was set to 0.75 Å – one-quarter of the highest resolution (3 Å) of data used. The Patterson vector length range used in the rotation search was 5–30 Å.

After calculating the correlation for every sampled search model orientation, the highest 6,000 peaks were chosen and clustered so that all peaks within 10° of each other in Eulerian angle space were represented by the single highest peak. This peak clustering process reduced the number of selected rotation peaks to around 100. To find the correct rotation solution from these peaks, Patterson correlation (PC) refinement (Brünger, 1990a) was used to refine the individual rotation peaks. During PC refinement, the search model was divided into two rigid body modules: domains I and IV as one and domains II and III as the other. The resolution range of the data used in both rotation search and PC refinement was 15–3 Å. The Patterson correlation value of the solution was found to be 6 times the standard deviation (σ) above the mean and 5σ above the next highest peak. A translation search with a search step of 1 Å using 10–3-Å-resolution data resulted in a solution with the structure factor correlation coefficient greater than 16σ above the mean, and about 9σ higher than the next highest peak. The initial R-factor of this solution was 53.1% at 10–3 Å. The same solution was also found by an independent Patterson search using routines in the program PROTEIN (Steigemann, 1991).

Table 1. *Refinement statistics*

Resolution (Å)	2.5
Total no. of observations	76,668
No. of the reflections	13,945
R_{sym}	5.35%
Completeness of data	97.3%
R-factor (10–2.5 Å, all data)	17.7%
No. of waters included	169
rms bond deviation (Å)	0.014
rms angle deviation (degrees)	2.7
Estimated coordinates error (Å) (from Luzzati plot)	0.2–0.3
Average B-factors (Å^2)	
Main chain	19
Side chain	22
Calcium ions	31
Solvent	37
Energy (kcal/mol)	−590

Refinement

The structure was refined using the program XPLOR by dividing the molecule into successively smaller rigid bodies. The model was initially divided into two modules; next each module was divided into the repeats; then each repeat was divided into two helix–loop–helix folds and one connecting helix; and finally individual helices were treated as rigid bodies. After each step of division, 20–50 cycles of conjugate gradient minimization at 6–3 Å resolution were performed. The R-factor after all steps of rigid body refinements was 43.8% for 6–3-Å-resolution data. Then 120 cycles of conventional positional refinement were performed, which reduced the R-factor to 34.6% at 6–3 Å.

At this point, a $2F_o - F_c$ map was calculated. About half of the missing side chains in the model were fitted into the electron density map. Another 100 cycles of positional refinement were done followed by refinement using a slow-cooling simulated annealing method (Brünger et al., 1990) with 5–2.5-Å-resolution data. This reduced the R-factor to 27.3%. A new $2F_o - F_c$ map allowed all the missing side chains to be fitted. Another round of refinements consisting of positional, simulated annealing, and individual B-factor refinement was performed, which lowered the R-factor to 22.9%. An omit map was calculated after deleting all the loop regions. All the loops were then rebuilt according to the omit map. Three of them (consisting of residues 30–33, 184–190, and 226–230) showed conformations substantially different from those of annexin V. The six amino-terminal residues were also fitted into the omit map at this time. The R-factor after rebuilding and refinement was 20.4% at 5–2.5 Å. At this stage, six calcium ions were clearly visible in the electron

density map. Incorporating these calciums into the model lowered the *R*-factor to 19.8%. Finally 169 water molecules were added. The present model has been refined to an *R*-factor of 17.7% at 10–2.5 Å resolution. The root mean square (rms) deviations of bond lengths and bond angles from ideality are 0.014 Å and 2.7°, respectively (Table 1). All refinement was done with the program XPLOR (Brünger, 1990b). The results of the refinement were confirmed by another independent refinement starting from the Patterson search solution obtained using the PROTEIN program.

Structure description

The current model of annexin I (Fig. 1) has the same overall topology as annexin V (Huber et al., 1990a,b, 1992). It consists of four structurally homologous domains and two connecting strands. Domains I, II, III, and IV are made up of residues 17–86, 87–158, 169–246, and 247–319, respectively. Residues 6–16 and 159–168 form the two connecting strands.

Each of the four domains can be described in the same way. There are five helices, namely A, B, C, D, and E. Helices A and B, and helices D and E form two parallel helix–loop–helix folds. Helix C, lying at the opposite side of the loops with its axis approximately perpendicular to the other four helices, connects the C-terminus of helix B to the N-terminus of helix D. Interdomain strand 1 has its amino-terminus noncovalently attached to domain IV, "linking" domains I and IV to form a two-domain module. Interdomain strand 2 covalently links domains II and III to form another two-domain module (Table 2). These two modules are related by a pseudo twofold axis (Fig. 1; Kinemage 1). The two domains within each module make tight hydrophobic contacts, while interactions between the two modules are made mostly by hydrophilic side chains.

The four domains pack together to form a slightly curved plate. All the loop regions of the helix–loop–helix folds are located at the convex face of the plate. The four C-helices and two connecting loops are found at the concave face. A hydrophilic channel is formed between the four domains. The channel runs perpendicularly through the middle of the plate in projection (Fig. 1). A disulfide bridge not present in annexin V was found in domain IV between residues Cys 297 and Cys 316.

All six calcium sites are found at the loop regions of the helix–loop–helix folds on the convex face of the molecule. These loops fall into two classes. One class is formed by the loops between the A and B helices (these will be referred to as the AB loops). The other class is composed of the loops between the D and E helices, and will be described as the DE loops. Thus, each of the four annexin I domains contains a copy of each class of loops. The AB loops are five to seven residues long, with sequence (K,R)-(G,R)-X-G-T. The DE loops are much shorter, with only one or two residues between the two helices (Table 2).

Discussion

Calcium binding sites

Six of the eight loops in the helix–loop–helix folds are found to have bound calcium ions. There are two classes of calcium binding sites in annexin I: type II and type III (type I referred to here is the well-known EF-hand calcium binding site). Whereas all the loops in annexin I that have the type II site conformation are found to have bound calcium ions, not all of the loops that have the type III site conformation are occupied by calcium ions. Type

Table 2. *Amino acid sequence arrangement of annexin I*

	Domain I	Domain II	Domain III	Domain IV
Helix A	17–30	87–100	169–182	247–260
Loop	31–33 (Ca^{2+})[a]	101–105 (Ca^{2+})	183–189 (Ca^{2+})	261–265 (Ca^{2+})
Helix B	34–45	106–117	190–201	266–277
				278, 279
Helix C	46–62	118–134	202–216	280–292
	63	135	217–219	293, 294
Helix D	64–72	136–145	220–229	295–304
Loop	73, 74 (Ca^{2+})	146	230	305 (Ca^{2+})
Helix E	75–86	147–158	231–246	306–318
				319

Connector I: 6–16
Connector II: 159–168

[a] The loops that bind calcium are indicated by (Ca^{2+}). All four loops between helices A and B contain calcium ions, whereas only two out of four loops between helices D and E bind calcium ions.

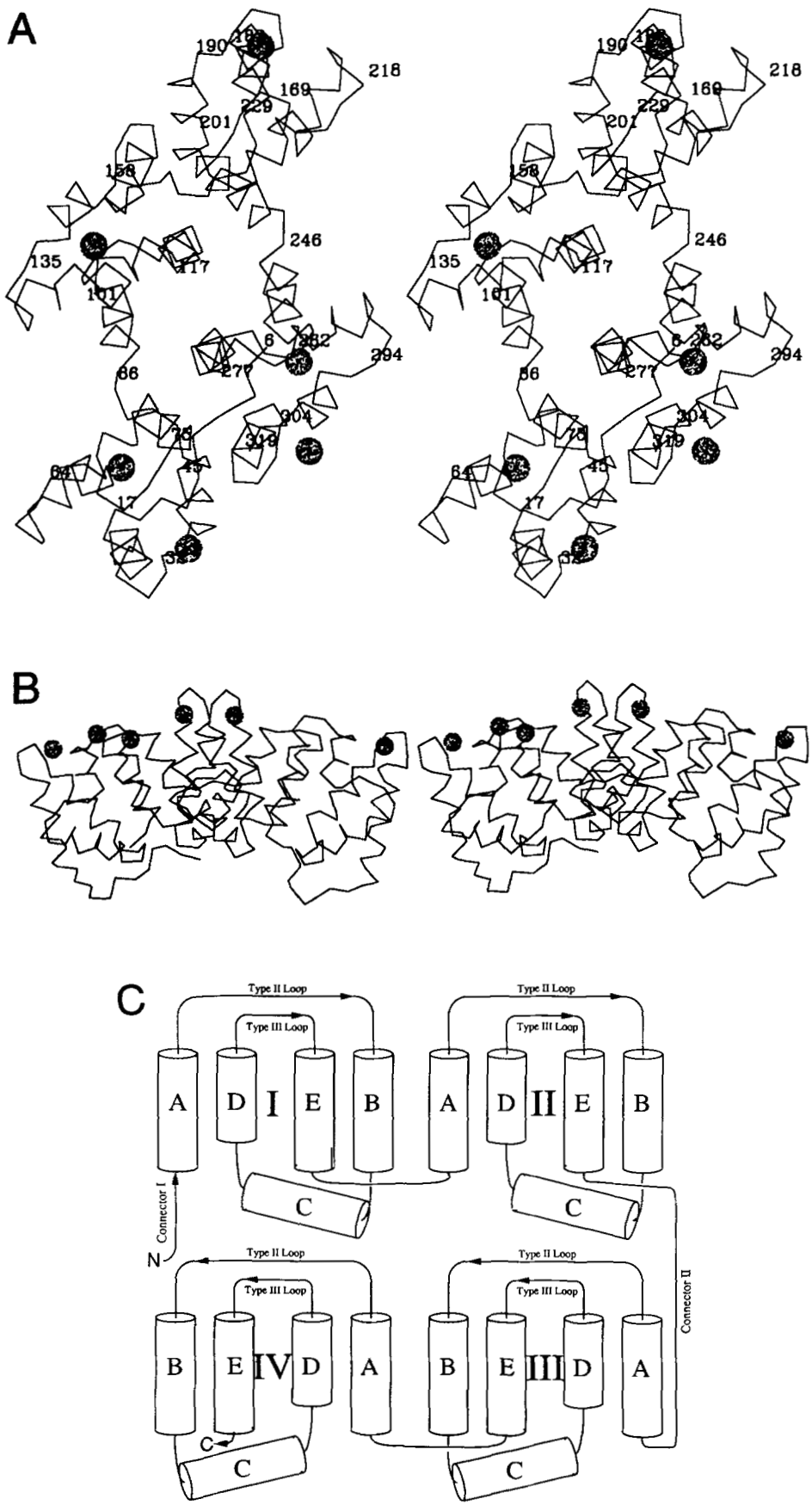

Fig. 1. Annexin 1. **A:** Top view. **B:** Side view. Six observed calciums are shown in A and B. **C:** Topological structure.

II calcium binding sites are found only at AB loops. The coordination of the type II sites is octahedral. It consists of three peptide oxygens from the AB loops with the (K,R)-(G,R)-X-G-T sequence and the bidentate ligands from the acidic group of either an aspartate or a glutamate 39 residues downstream in the sequence (Figs. 2A, 3B; Kinemage 2). This residue has been referred to as the "cap" residue (Huber et al., 1990b) (Tables 3, 4). The remaining two calcium coordinating sites show electron density for water molecules. The type II sites are similar to the phospholipid binding site of phospholipase A2 (Verheij et al., 1980; Huber et al., 1990b). The calcium ions at the type III sites coordinate to two backbone carbonyl oxygens and one nearby acidic side chain (Cap) (Figs. 2B, 3C; Kinemage 3; Table 3). Water molecules have been found at most of the remaining three coordinating sites to complete the six-ligand octahedral coordination. The type III sites correspond to the two minor calcium sites labeled by lanthanum in annexin V (Huber et al., 1990b). The average calcium ligand distance for both type II and type III sites is 2.6 Å.

Neither the type II nor the type III calcium binding sites belong to the well-characterized EF-hand calcium binding motif (Weinman, 1991). The EF-hand motif (type I), first identified in the crystal structure of a parvalbumin (Moews & Kretsinger, 1975), consists of a 12-residue calcium binding loop between two helices. Four to six loop residues containing oxygen atoms in their side chains, and a backbone carbonyl group are coordinated to calcium (Fig. 3A). As described above, the two calcium binding motifs found in annexin I (type II and type III) involve much shorter loops. Only part of the calcium ligands are provided by the protein molecule, and water molecules complete the coordination.

Table 3. *Calcium ligands*

	Backbone carbonyls	Side-chain carboxyls
Ca^{2+} 1 (III(AB))	Gly 32, Val 33	Glu 35 O_ε^1, O_ε^2
Ca^{2+} 2 (III)	Lys 70, Leu 73	Glu 78 O_ε^1
Ca^{2+} 3 (II)	Met 100, Gly 102, Gly 104	Asp 144 O_δ^1, O_δ^2
Ca^{2+} 4 (II)	Gly 183, Arg 186, Gly 188	Glu 228 O_ε^1, O_ε^2
Ca^{2+} 5 (II)	Met 259, Gly 261, Gly 263	Glu 303 O_ε^1, O_ε^2
Ca^{2+} 6 (III)	Leu 301, Thr 304	Glu 309 O_ε^1

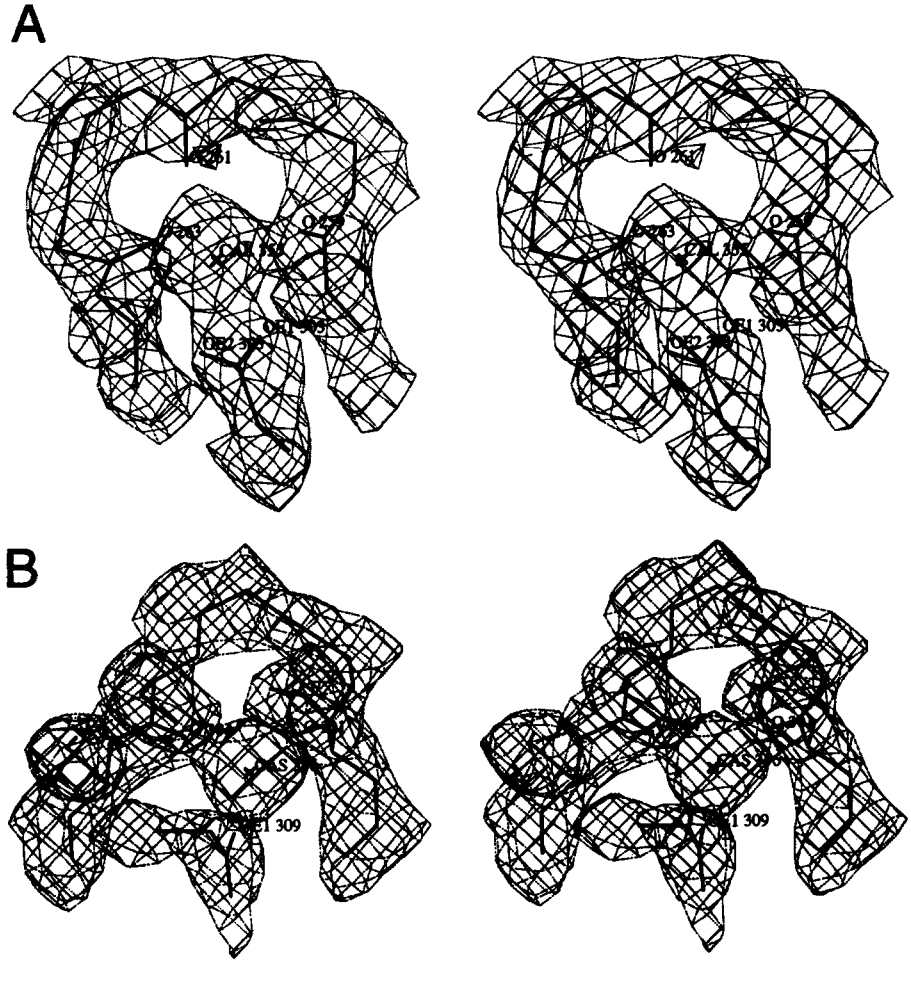

Fig. 2. $2F_o - F_c$ electron density map of the type II (**A**) and type III (**B**) calcium binding sites in domain IV. Map contoured at 1.0σ. Calciums and their ligands are labeled.

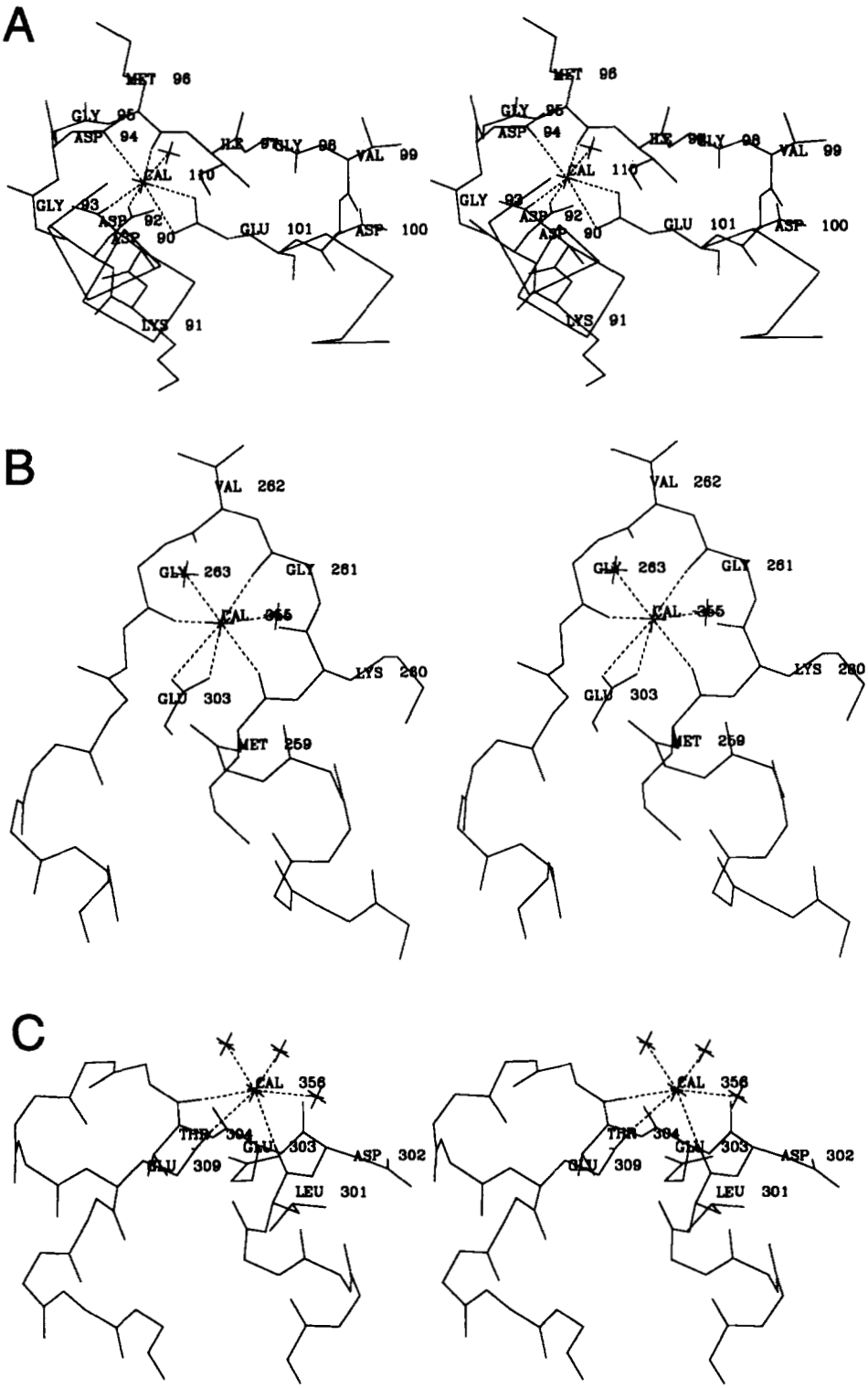

Fig. 3. Comparison of three types of calcium binding site. **A:** Type I (EF-hand) calcium binding site of parvalbumin (extracted from Protein Data Bank file 3pal.pdb). **B:** Type II. **C:** Type III calcium binding site in domain IV of annexin I.

As mentioned above, all type II sites are located at the AB loops. Three of the six calcium ions occupy the type II sites in domains II, III, and IV. The superposition of all four AB loops (Fig. 4A) shows that the type II sites of domains II and IV are very similar. Although the AB loop in domain III has one more residue, it still has the type II site calcium binding geometry. The AB loop in domain I is an exception. Instead of forming a type II site like the other AB loops, the AB loop of domain I binds a calcium ion in a manner similar to that described for the type III sites, with two backbone oxygens and a nearby glutamate. We call this unusual site type III(AB). This ex-

Table 4. *Comparison of calcium binding sites between annexin I and V*

Annexin	Domain	AB loop						Cap for type			Ca^{2+} sites		
								II	III(AB)	III	II	III(AB)	III
		28	29	30	31	32	33	72	35	78			
I	V	I	M	V	K	G	V	A	E	E		+	+
V	1	M	K	G	L	G	T	E	E	E	+	+	+
		100	101	102	103	104	105	144	107	150			
I	2	M	K	G	L	G	T	D	E	R	+		
V	2	L	K	G	A	G	T	D	E	Q	+		
		184	185	186	187	188	189	228	191	234			
I	3	E	R	R	K	G	T	E	V	E	+		
V	3	E	L	K	W	G	T	E	E	E			
		259	260	261	262	263	264	303	266	309			
I	4	M	K	G	V	G	T	E	H	E	+		+
V	4	M	K	G	A	G	T	D	D	K	+		

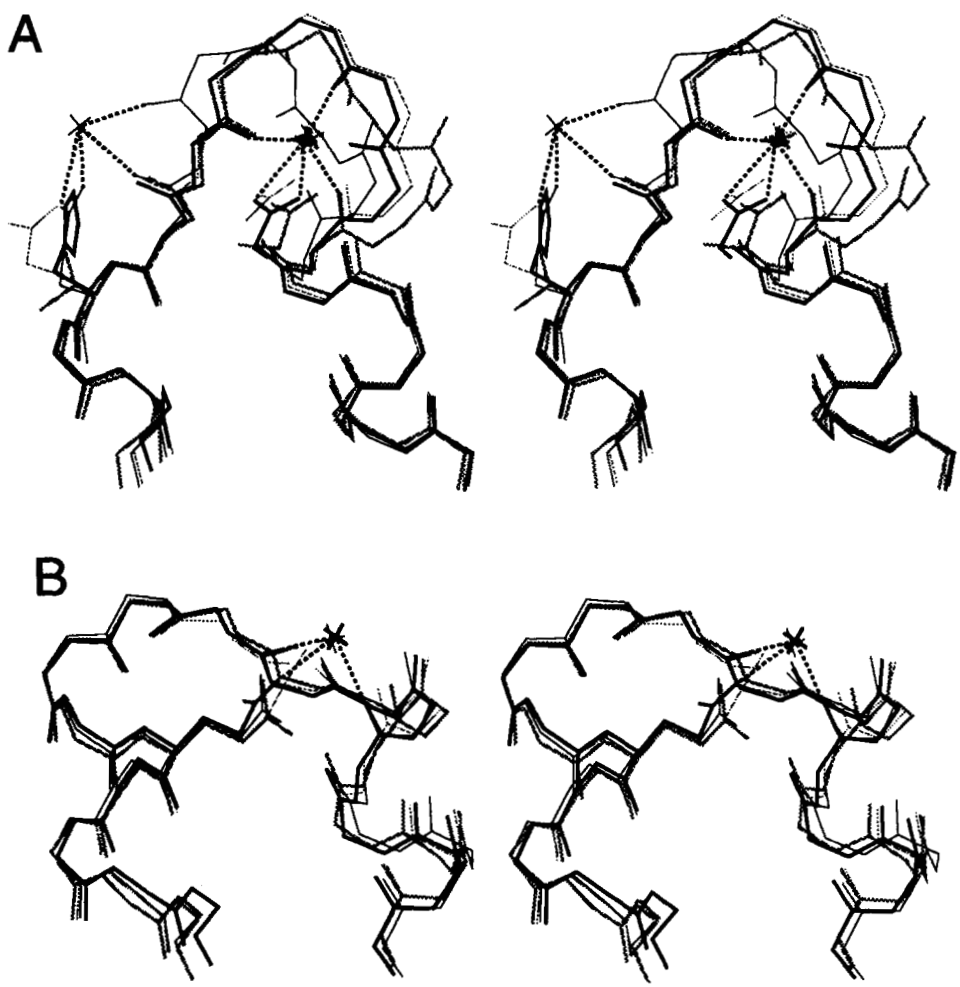

Fig. 4. Superpositions of all four AB loops (**A**) and all four DE loops (**B**) of annexin I. Thin black, thin gray, thick gray, and thick black lines represent domains I, II, III, and IV, respectively. Notice that the AB loop of domain I is different from the other three: it forms the exceptional type III(AB) site instead of the type II site.

ception is due to the absence of the required negatively charged cap residue 39 residues downstream from the AB loop. The DE loops in domains I and IV form type III sites that bind the other two calcium ions. The superposition of all four DE loops (Fig. 4B) shows that they have almost identical backbone conformations. In domain II, an arginine has replaced the required acidic cap residue near the DE loop (Table 4). This could be the reason that the DE loop of domain II fails to bind a calcium ion. The DE loop of domain III forms a typical type III site complete with the "cap" residue (Fig. 4B). It is unclear to us why this loop fails to bind calcium.

Structure comparison

A backbone superposition of the annexin V structure with annexin I results in an rms deviation of 2.34 Å (Fig. 5; Table 5). The largest differences are at the three regions that required retracing during the refinement (Fig. 6).

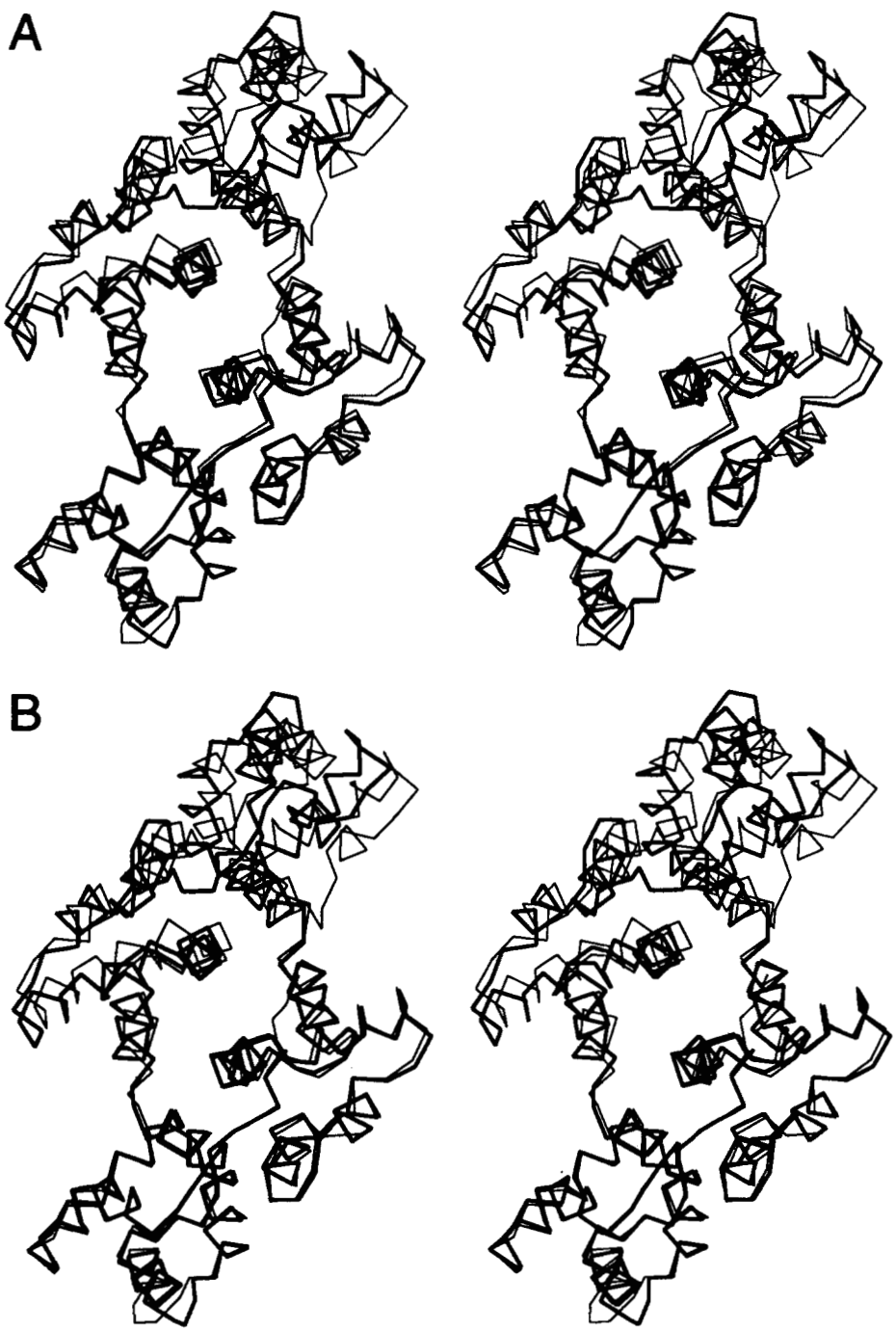

Fig. 5. C_α drawings of the superposition of annexin I (thick lines) and annexin V (thin lines). **A:** Superposition of backbone atoms of helices of domain I. **B:** Superposition of backbone atoms of helices of domains I and IV.

Table 5. *Root mean square deviations of backbone atoms of helices in different superpositions*[a]

Superposed domain	rms between domain I's	rms between domain II's	rms between domain III's	rms between domain IV's	rms between molecules
A. Superpositions of backbone atoms of helices of each domain of annexins I and V					
I	0.51	1.63	3.32	1.07	1.96
II	3.02	0.85	1.94	1.37	1.96
III	9.09	2.65	1.31	5.11	5.36
IV	0.69	2.14	4.34	0.63	2.49
Superposed domains	**rms between I+II's**	**rms between III+IV's**	**rms between II+III's**	**rms between I+IV's**	**rms between molecules**
B. Superpositions of backbone atoms of helices of two out of four domains					
I+II	1.02	2.22			2.54
III+IV	2.10	1.60			2.49
II+III			1.35	3.82	3.22
I+IV			3.24	0.61	3.09

[a] All units are Å.

One of the three largest differences is found at residues 184–190. The residues are in the AB loop of domain III. In annexin I, this loop forms a new type II calcium binding site not seen in annexin V (Huber et al., 1990b). Trp 187 in annexin V has a C_α displacement of 10.0 Å with respect to the corresponding annexin I residue Lys 187. The location of this tryptophan in annexin V prevents the type II binding loop of domain III from being formed in annexin V.

The DE loops of domain III are also quite different between annexins I and V. Although no new calcium ion was found at this loop, residues 226–230 in annexin I have adopted a type III site conformation. In annexin V, helix IIID is exceptionally short because the three consecutive charged residues Asp 226, Arg 227, and Glu 228 cannot be accommodated in helical geometry (Huber et al., 1990a). Also Glu 228 of annexin V has a 16.9-Å displacement with respect to Glu 228 in annexin I. This is a consequence of the distorted type II site in the same domain caused by Trp 187, as mentioned above. The exceptionally short helix IIID and the large displacement of Glu 228 are the reasons why annexin V failed to form a type III site at the DE loop of domain III. The change from Arg 227 in annexin V to Leu 227 in annexin I allows helix D in domain III to be extended in annexin I. The properly formed type II site in annexin I also makes the proper formation of helix IIID feasible. The DE loop in annexin I then forms a regular type III site.

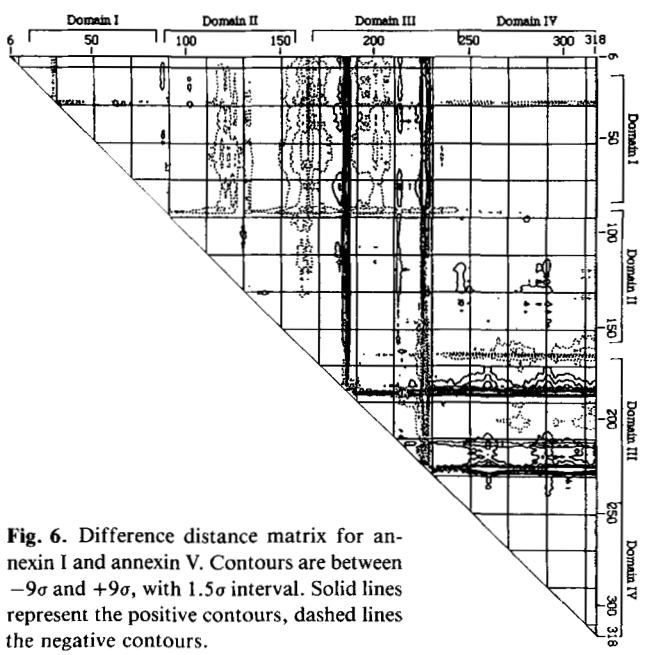

Fig. 6. Difference distance matrix for annexin I and annexin V. Contours are between -9σ and $+9\sigma$, with 1.5σ interval. Solid lines represent the positive contours, dashed lines the negative contours.

The third difference is at the AB loops of domain I. In annexin I, this loop binds one calcium ion in a type III(AB) site conformation instead of the type II site conformation. In annexin V, two calcium ions are bound to the same loop: one is in a type II site and the other is in a type III(AB) site. The lack of a type II site in domain I is due to the absence of the required negatively charged cap residue 39 residues downstream.

At the channel region between the four repeats, main chain and side chain conformations of annexin I and V superimpose very well. Several trapped water molecules move less than 0.5 Å. Salt-bridges in this region are also conserved: Asp 92–Arg 117 and Asp 280–Arg 276 on the concave end, and Lys 267 (His in annexin V)–Glu 95–Arg 271–Glu 112 on the convex end (Fig. 7).

Implication for biological function

All the calcium binding loops are found at the convex face of the annexin I molecule. Type II loops are similar to the

Fig. 7. Hydrophilic interact region between two modules of annexin I. Conserved salt bridges are highlighted.

phospholipid binding site in phospholipase A2 (Verheij et al., 1980; Huber et al., 1990b), adding to other arguments that annexins bind membrane lipids at the convex face (Brisson et al., 1991). The similarity between the type II loops and the phospholipid binding sites in phospholipase A2 also supports the idea that the phospholipase A2 inhibitory activity of annexin I is due to an interaction of annexin I with phospholipid substrates rather than with the enzyme (Dennis & Davidson, 1990).

The EF-hand (type I) motif sequesters calcium almost completely, whereas the annexin I calcium binding loops are more open to allow binding of phospholipid to the calcium. The coordinating water molecules may be replaced by phospholipids. Sequence alignment shows that the calcium binding loop regions are highly conserved in the annexin family. This indicates that the two calcium binding motifs we observed in annexin I and V are universal within the annexin family.

The N-terminal region of annexin I can be phosphorylated by the epidermal growth factor receptor kinase. Experiments have shown that annexin I has enhanced calcium sensitivity for phospholipid binding after proteolysis or phosphorylation at the N-terminal region (Schlaepfer & Haigler, 1987; Ando et al., 1989) suggesting that the N-terminal region has regulatory function for lipid binding. Although the specific site of phosphorylation (Tyr 21 in annexin I numbering) is not present in the annexin I molecule we report here, it is most likely located at the concave face of the molecule, possibly close to the opening of the hydrophilic channel. Phosphorylation may alter the position of the N-terminal and induce conformational changes or alter equilibrium, affecting calcium and phospholipid binding at the opposite face of the molecule.

Materials and methods

A cDNA library was constructed from human placenta and screened using a 30-nucleotide-long probe containing a portion of the sequence of annexin I cDNA from human cell line U937 (Wallner & Mattaliano, 1986). Colonies positive for annexin I were identified, and DNA sequences of the plasmids from these colonies determined. The sequences were identical to the published sequence except for one silent nucleotide change from T to G at position 288, corresponding to the 96th amino acid. Plasmid pHT12I containing a *trc* promoter, which was used as the expression vector, was kindly provided by Dr. Hideki Tachibana of Kobe University, Kobe, Japan. An annexin I clone lacking the amino-terminal 31 residues gave high expression of the protein. This protein showed in vitro phospholipase A2 inhibition, like the nontruncated form, but was more easily purified.

The soluble fraction of the expressed protein was purified as follows. Cells were sonicated in 25 mM Tris buffer, 1 mM EDTA, pH 8.5. The soluble fraction was obtained by centrifugation, and 10% glycerol by volume was added. The fraction was loaded on a DE-52 (Whatman) anion exchange column and the flow-through fraction was collected and concentrated by ultrafiltration. The buffer was changed to 25 mM Tris at pH 9.3 with 1 mM EDTA, the sample was loaded onto the DE-52 column, and the fraction corresponding to the salt gradient from 0 to 0.3 M NaCl was collected and concentrated by ultrafiltration. The buffer was changed to 25 mM Tris at pH 7.7, 1 mM EDTA, and 0.1 M NaCl, in which the protein was finally purified on a Sephacryl S200 (Pharmacia) column. Some of the batches were further purified by hydroxyl apatite chromatography. The protein was kept in a soluble state during the entire purification procedure.

The protein was screened for crystallization conditions in the presence and absence of Ca^{2+} by the sparse matrix method (Jancarik & Kim, 1991). In the presence of calcium ions, the best crystals grew from 14-μL drops of 20 mg protein/mL solution containing 0.05 M cacodylate buffer at pH 6.5, 0.1 M Na(OAc), 10 mM $CaCl_2$, and 8% PEG 4000 equilibrated against 0.1 M cacodylate, 0.2 M Na(OAc), 10 mM $CaCl_2$, and 16% PEG 4000 at the same pH and room temperature. Crystals grow as hexagonal plates and have typical dimensions of 1.0 × 0.6 × 0.4 mm. The crystals have the space group $P2_12_12_1$, with cell dimensions of a = 139.36 Å, b = 67.50 Å, and c = 42.11 Å. The unit cell contains one molecule in the asymmetric unit. This crystal form diffracts to 2.5 Å resolution.

Acknowledgments

We thank Hay Young Lee, Dr. Soonhee Park, and Dr. Vincent Powers for helping with the preparation and purification of the protein; Jamila Jancarik for the crystallization; Andrew Bohm, Dr. J. Pandit, Dr. Gil Privé, Dr. Mike Milburn, Prof. N. Sakabe, Dr. A. Nakagawa, and N. Watanabe for X-ray diffraction data collection at Photon Factory, Tsukuba, Japan; and Dr. Steve Holbrook, Andrew Bohm, John Somoza, and Dr. Bill Scott for critical reading and comments on the manuscript. This work has been supported by grants from the Ministry of Science and Technology, Saehan Pharmaceutical Co., Asan Foundation, Seoul, Korea (to D.S.K.), the U.S. Department of Energy, and the U.S. National Science Foundation (to S.-H. K.).

References

Ando, Y., Imamura, S., Hong, Y.M., Owada, M.K., Kakunaga, T., & Kannagi, R. (1989). Enhancement of calcium sensitivity of lipocortin I in phospholipid binding induced by limited proteolysis and phosphorylation at terminus as analyzed by phospholipid affinity column. *J. Biol. Chem. 264*, 6948–6955.

Brisson, A., Mosser, G., & Huber, R. (1991). Structure of soluble and membrane-bound human annexin V. *J. Mol. Biol. 220*, 199–203.

Brünger, A.T. (1990a). Extension of molecular replacement—A new search strategy based on Patterson correlation refinement. *Acta Crystallogr. Sect. A 46*, 46–57.

Brünger, A.T. (1990b). XPLOR: A system for crystallography and NMR. Version 2.1.

Brünger, A.T., Krukowski, A., & Erickson, J.W. (1990). Slow-cooling protocols for crystallographic refinement by simulated annealing. *Acta Crystallogr. Sect. A 46*, 585–593.

Crompton, M.R., Moss, S.E., & Crumpton, M.J. (1988). Diversity in the lipocortin/calpactin family. *Cell 55*, 1–3.

Dennis, E.A. & Davidson, F.F. (1990). Phospholipase A2 and lipocortin effects. *Prog. Clin. Biol. Res. 349*(47), 47–54.

Ernst, J.D., Hoye, E., Blackwood, R.A., & Mok, T.L. (1991). Identification of a domain that mediates vesicle aggregation functional diversity of annexin repeats. *J. Biol. Chem. 266*, 6670–6673.

Flower, R.J. (1988). Eleventh Gaddum Memorial Lecture. Lipocortin and the mechanism of action of the glucocorticoids. *Br. J. Pharmacol. 94*, 987–1015.

Glenney, J. & Tack, B. (1985). Amino-terminal sequence of p36 and associated p10: Identification of the site of tyrosine phosphorylation and homology with S-100. *Proc. Natl. Acad. Sci. USA 82*, 7884–7888.

Glenney, J. & Zokas, L. (1988). Antibodies to the N-terminus of calpactin II (p35) affect Ca^{2+} and phosphorylation by the epidermal growth factor receptor in vitro. *Biochemistry 27*, 2069–2076.

Haigler, H.T., Schlaepfer, D.D., & Burgess, W.H. (1987). Characterization of lipocortin I and an immunologically protein as epidermal growth factor receptor/kinase substrates and phospholipase A2 inhibitors. *J. Biol. Chem. 262*, 6921–6930.

Higashi, T. (1989). The processing of diffraction data taken on a screenless Weissenberg camera for macromolecular crystallography. *J. Appl. Crystallogr. 22*, 9–18.

Huber, R. (1985). Molecular replacement. In *Proceedings of the Daresbury Study Weekend* (Machin, P.A., Ed.), pp. 58–61. Science and Engineering Research Council, The Librarian, Daresbury Laboratory, Daresbury, UK.

Huber, R., Berendes, R., Burger, A., Schneider, M., Karshikov, A., Luecke, H., Römisch, J., & Paques, E. (1992). Crystal and molecular structure of human annexin V after refinement. *J. Mol. Biol. 223*, 683–704.

Huber, R., Römisch, J., & Paques, E.P. (1990a). The crystal and molecular structure of human annexin V, an anticoagulant protein that binds to calcium and membranes. *EMBO J. 9*, 3867–3874.

Huber, R., Schneider, M., Mayr, I., Römisch, J., & Paques, E.P. (1990b). The calcium binding sites in human annexin V by crystal structure analysis at 2.0 Å resolution. Implications for membrane binding and calcium channel activity. *FEBS Lett. 275*, 15–21.

Jancarik, J. & Kim, S. (1991). Sparse matrix sampling—A screening method for crystallization of proteins. *J. Appl. Crystallogr. 24*, 409–411.

Karshikov, A., Berendes, R., Burger, A., Cavalie, A., Lux, H.-D., & Juber, R. (1992). Annexin V membrane interaction: An electrostatic potential study. *Eur. Biophys. J. 20*, 337–344.

Klee, C.B. (1988). Ca^{2+}-dependent phospholipid- (and membrane-) binding proteins. *Biochemistry 27*, 6645–6653.

Moews, P.C. & Kretsinger, R.H. (1975). Refinement of the structure of carp muscle calcium-binding parvalbumin by model building and difference Fourier analysis. *J. Mol. Biol. 91*, 201–228.

Peers, S.H. & Flower, R.J. (1990). The role of lipocortin in corticosteroid actions. *Am. Rev. Respir. Dis. 141*, S18–S21.

Rossmann, M.G. (1972). *The Molecular Replacement Method* (L. Klein, L., Ed.). International Science Review Series. Gordon and Breach, Science Publishers, New York.

Sakabe, N. (1983). A focusing Weissenberg camera with multi-layer-line screens for macromolecular crystallography. *J. Appl. Crystallogr. 16*, 542–547.

Schlaepfer, D.D. & Haigler, H.T. (1987). Characterization of Ca^{2+}-dependent phospholipid binding and phosphorylation of lipocortin I. *J. Biol. Chem. 262*, 6931–6937.

Steigemann, W. (1991). PROTEIN: A program system for the crystal structure analysis of proteins. Version 3.1.

Verheij, H.M., Volweik, J.J., Jansen, E.H.J.M., Puyk, W.C., Gijkstra, B.W., Drenth, J., & de Haas, G.H. (1980). Methylation of histidine-48 in pancreatic phospholipase A2. Role of histidine and calcium ion in the catalytic mechanism. *Biochemistry 19*, 743–750.

Wallner, B.P. & Mattaliano, R.J. (1986). Cloning and expression of human lipocortin, a phospholipase A2 inhibitor with potential anti-inflammatory activity. *Nature 320*, 77–81.

Weinman, S. (1991). Calcium-binding proteins: An overview. *J. Biol. Buccale 19*(1), 90–98.